Peer reviewed version

Link to published version (if available):
10.1260/1756-8293.7.3.275

Link to publication record on the Bristol Research Portal
PDF-document

University of Bristol – Bristol Research Portal
General rights

The energy benefits of the pantograph wing mechanism in flapping flight: case study of a gull

∗**Burgess, S.C., *Lock, R.J., *Wang, J., $Sattler, G.D. and $Oliver, J.D.**

*Department of Mechanical Engineering, Bristol University, UK

$Department of Biology and Chemistry, Liberty University, US

Abstract

Bird wings generally contain a 4-bar pantograph mechanism in the forearm that enables the wrist joint to be actuated from the elbow joint thus reducing the number of wing muscles and hence reducing the wing inertia and inertial drag. In this paper we develop a theoretical model of inertial power for flapping flight to estimate the advantage of the 4-bar pantograph mechanism by comparing the inertial power required for the case where wrist muscles are present in the forearm with the case where wrist muscles are not present in the forearm. It is difficult to predict how wrist muscles would look when there is no pantograph mechanism. Therefore a lower bound and upper bound case are defined. The lower bound case involves redistributing the elbow muscles with no increase in wing mass. The upper bound case involves replicating the biceps-triceps muscles near the wrist joint. At minimum power speed the model estimates that the 4-bar pantograph mechanism reduces the inertial power for the gull from between 6.1%-12.3% and reduces the overall power by 0.6%-1.2%. When account is taken of the tight margins involved in the design of a flying vehicle, the energy savings produced by the pantograph mechanism are significant. A ring-billed gull was chosen for the case study and an adult specimen was obtained to gather morphometric data. Lessons for the design of flapping micro air vehicles are discussed.

1. INTRODUCTION

During level flapping bird flight, four main contributions to energy are encountered: induced drag, body drag, wing profile drag and wing inertial drag. Flapping flight requires a large amount of inertial power because flapping occurs at high frequencies, typically between 3Hz to 30Hz (Pennycuick 1996). Bird wings benefit from having a low inertia in order to minimise the inertial power requirements (Norberg 1990). The inertia of bird wings is low due to a skeletal structure made from bone with high strength-to-weight and stiffness-to-weight ratios, along with multi-link lightweight feathers (Dumont 2010). In addition, the wing inertia is minimised with a mechanism in the forearm section of the wing which enables the bicep and triceps muscles to actuate the wrist joint through actuation of the elbow joint. This reduces the number of muscles in the forearm section of the wing and hence reduces the wing inertia. The multi-link mechanism in the wing can be modelled as a pantograph mechanism (Norberg 1990). The pantograph articulates the wing in a controlled manner, whereby the torque input into the root hinge (the elbow joint) causes the parallelogram to open and close, which in turn deploys or retracts the wing.

In this paper we develop a theoretical model of inertial power for flapping flight to estimate the advantage of the 4-bar pantograph mechanism by comparing the inertial power required for the case where wrist muscles are present in the forearm with the case where wrist muscles are not present in the forearm. A ring-billed gull was chosen for the case study because it is a common medium-sized bird that is an efficient flyer. The ring-billed gull (*Larus delawarensis*) is one of the most common birds in North America and is able to migrate thousands of miles each winter on journeys such as from North America to Europe.

Reduction of the inertia of wings and limbs is of interest to engineers for the design of flapping micro air vehicles (FMAVs). Birds are extremely well optimised for flight and so it is important to understand the features that contribute to optimal design in order to create efficient FMAVs. Recent studies have shown that birds take advantage of automatic aerodynamic braking due to the very low inertia of their wings and this can be used to design efficient FMAVs (Burgess et al. 2014). The relevance of the pantograph mechanism for FMAV design is discussed in this paper.

2. THE PANTOGRAPH 4-BAR MECHANISM IN BIRD WINGS
2.1 Description of the bird wing

Figure 1 shows a skeletal and simplified schematic representation of the pantograph wing mechanism of birds. The bird wing consists of humerus, radius, ulnare and radiale bones as well as a group of smaller bones which make up the hand section (Nudds, et al 2007; Videler, 2005). Flapping flight in birds consists of four basic motions: flapping, feathering, lead-lagging and spanning (Tobalske & Dial 1996). The motion shown in Figure 1 is that of spanning. Spanning motion has two main functions. Firstly, it enables a bird to retract its wings for stowage on the ground. Secondly, it enables the bird to adjust wing span during flight for performing flight manoeuvres; skills that would be of use to MAVs.

2.2 Description of the 4-bar pantograph mechanism

The radius and ulna connect with ends of the humerus and wrist bone to form the pantograph 4-bar mechanism. The radius and ulna form the long bars, and the end of the humerus and wrist bones are the short bars (Meyers & Mathias 1997). A four-bar mechanism is possible because, unlike the elbow joints of mammals, in the bird wing both the ulnare and radius have two individual points of articulation where they join the humerus and also two points of articulation where they meet the wrist (Nudds et al. 2007; Meyers & Mathias 1997). This means that in the case of bird wings there are four points of articulation in the forearm and hence enough points of rotation for a 4-bar mechanism. The 4-bar mechanism causes the elbow and wrist joints to be constrained and to move together in a coupled way. Rotation at the elbow joint causes the same rotation at the wrist joint.

Birds are not the only creature to use a 4-bar mechanism to optimise an actuation function. The sling jaw wrasse has a 4-bar parallelogram mechanism for deploying a mouth at high speed (Burgess et al. 2011) and the mammalian knee joint has an inverted 4-bar mechanism for creating a rolling/sliding joint (Etoundi et al. 2011).
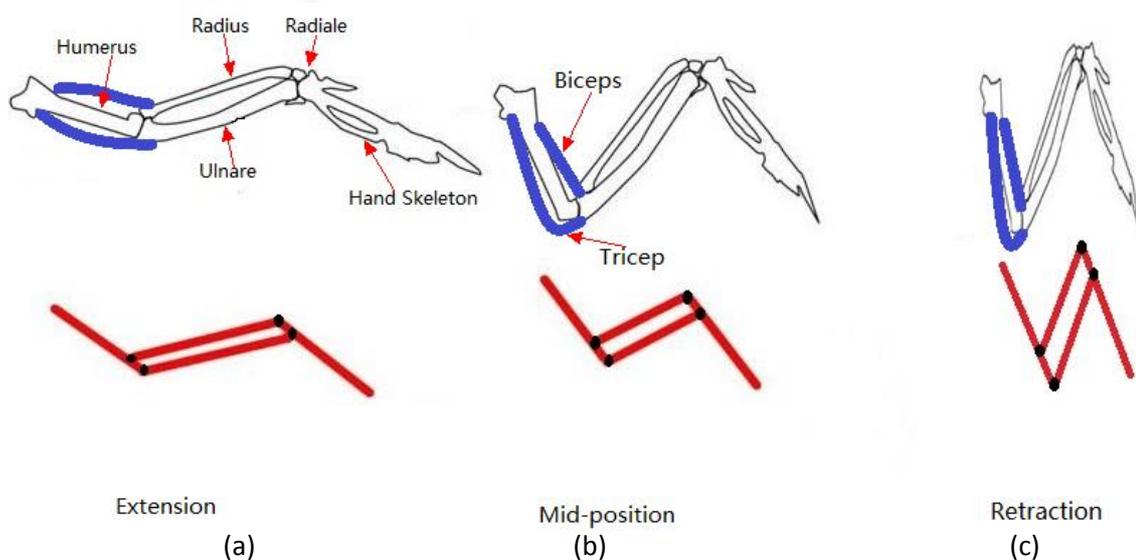

Figure 1. Anatomy of bird wing (a) deployed (b) partially retracted (c) retracted (adapted from Pennycuick 2008)

2.3 Purpose of the 4-bar pantograph mechanism

One key function of the 4-bar mechanism is to remove the need for wrist muscles at the wrist joint by coupling the elbow and wrist joint together (Norberg 1990). A second function of the 4-bar mechanism may be to constrain the way the wing deploys in order to simplify the control of flight. The advantages of having this constrained co-ordinated motion is that when the wing is partially retracted for flight manoeuvres such as fast gliding, the profile and hence drag coefficient of the two wings are consistent. A problem with having independent elbow and wrist joints would be that the shape of the wing would be highly variable and the drag coefficient would vary greatly, thus making flight manoeuvres more difficult to control. A third function of the 4-bar mechanism may be to make wing retraction easier. It is less effort for the birds to keep wings retracted because there are fewer muscles to restrain. So it is probable that the 4-bar mechanism has multiple functions. Multi-functioning is common in natural systems (Burgess 2007; Burgess et al. 2006).

2.4 Dissection of 4-bar pantograph mechanism

A ring-billed gull was carefully dissected to reveal the 4-bar mechanism (skin removed but ligaments and muscles in-tact). With the humerus exposed it was possible to fully deploy and retract the wing just by moving the humerus bone as shown in Fig. 2. This experiment demonstrated the simplified assumption that a 4-bar mechanism within the wing functioned as Norberg stated (Norberg 1990). It should be noted that this is an obvious simplification of the full avian wing physiology but provides evidence of the main mechanism in action, which the authors believe would be of use in FMAV design.
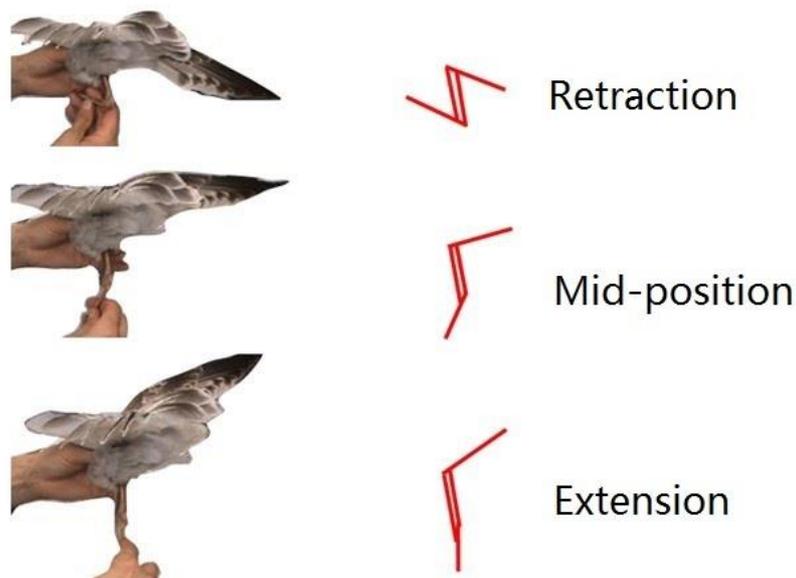

Figure 2. Demonstration of the wing 4-bar pantograph mechanism

3. ESTIMATION OF INCREASED WING INERTIA WHEN 4-BAR MECHANISM IS NOT PRESENT

It is difficult to predict how the muscle mass at the elbow joint and wrist joint would differ for the case where there is no 4-bar pantograph mechanism. Whilst it is clear that the wrist joint muscle mass would increase, it is difficult to predict by how much and it is not clear if the biceps-triceps muscle mass would change. Therefore a lower bound and upper bound case are defined. The lower bound case involves redistributing the elbow muscles with no increase in wing mass. The upper bound case involves replicating the biceps-triceps muscle near the wrist joint thus increasing the wing mass. This is analogous with having a driving mechanism (in this case muscle) placed out on the wing of an FMAV to enable wing morphing in flight.

It is very difficult to predict the additional inertia if there were wrist muscles so a lower and upper bound were estimated based on conservative assumptions.

3.1 Lower bound (LB) estimate of increased wing inertia

For the lower bound estimate of increased wing inertia, wrist muscles were added to the wrist joint by splitting the original biceps-triceps muscles, leaving one half at the current location (elbow joint) and putting one half at the wrist joint. In this scenario the total wing mass is unchanged.

The position of the biceps-triceps muscles was obtained by carefully removing the feathers and skin to reveal the muscles as shown in Fig. 3. The radius for the biceps-triceps muscles $r_{b\text{-}t}$ from the centre of rotation of the shoulder joint to the centre of mass of the biceps-triceps muscle was measured to be 40 mm.

Figure 3. Photograph of biceps-triceps muscles

A single set of biceps-triceps muscles were measured to weigh $m_{b\text{-}t}$ = 4.3g for the ring-billed gull. Therefore, for the lower bound case, the mass of the biceps-triceps muscles was assumed to be $m_{b\text{-}t(LB)}$ = 2.15g and the mass of the wrist muscles was assumed to be $m_{r\text{-}m(LB)}$ = 2.15g. The distance from the shoulder joint to the elbow joint was measured to be 95mm. By making an assumption that the wrist muscle extended beyond the elbow joint by the same amount that the biceps muscle extended beyond the shoulder joint (i.e. 40mm) the estimated radius of the wrist muscles was $r_{w\text{-}m}$ = 135mm.

The increase in inertia of the wing ΔI_{LB} for the lower bound case is given by:

$$\Delta I_{LB} = m_{w-m(LB)} r_{w-m}{}^2 - 0.5 m_{b-t} r_{b-t}{}^2 \tag{1}$$

3.2 Upper bound (UB) estimate of wing inertia
For the upper bound case, the biceps-triceps muscles were estimated to be the same as the existing bird and the wrist muscles were assumed to have a mass equal to the elbow muscles i.e. $m_{w\text{-}m(UB)}$ = 4.3g. In this scenario the mass of the bird was increased by an amount equal to two sets of triceps-biceps muscles. As with the lower bound case, the estimated radius of the wrist muscles was $r_{w\text{-}m}$ = 135mm.

The increase in inertia of the wing for the gull for the upper bound case is given by:

$$\Delta I_{UB} = m_{w-m(UB)} r_{w-m}{}^2 \tag{2}$$

4. SUMMARY OF PHYSICAL DATA

The physical data used in this paper is summarised in Table 1. The wing inertia (with pantograph mechanism), was calculated from the equation $I = m_w r_g^2$ where m_w is the wing mass and r_g is the radius of gyration. The radius of gyration was taken as 0.317 L_w. This value of radius of gyration was measured by Berg and Rayner for a black headed gull of similar size (b= 0.93m) (Berg and Rayner, 1995). The total wing excursion angle during flapping was calculated from the equation $\phi = 1.1048 m_b^{-0.119}$ (Scholey, 1983). The flapping frequency was obtained from the empirical equation $f = m_b^{3/8} g^{1/2} b^{-23/24} S^{-1/3} \rho^{-3/8}$ (Pennycuick, 1996).

Wing characteristic	Term	Value	Source
Wing span (m)	b	1.03	Measured
Wing length	w_L	0.48	Measured
Mean wing width (m)	C_w	0.115	Measured
Single wing area $\times 10^{-4}$ (m²)	S	460	Measured
Bird mass (kg)	m_b	0.3515	Measured
Wing mass $\times 10^{-3}$ (kg)	m_w	32	Measured
Mass of b-t muscle $\times 10^{-3}$ (kg)	$m_{b\text{-}t}$	4.3	Measured
Distance to b-t muscles (m)	$r_{b\text{-}t}$	0.040	Measured
Distance to wrist muscles (m)	$r_{w\text{-}m}$	0.135	Estimated
Flapping frequency (Hz)	f	4.26	[Pennycuick 1996]
Total wing excursion angle (º)	ϕ	71.7	[Scholey 1983]
Flapping amplitude (rad)	γ	0.6257	
Wing inertia $\times 10^6$ (kgm²) (with 4-bar mechanism)	I	740.89	Derived
Wing inertia $\times 10^6$ (kgm²) (without 4-bar mechanism) LB	I'_{LB}	776.6	$I + \Delta I_{LB}$
Wing inertia $\times 10^6$ (kgm²) (without 4-bar mechanism) UB	I'_{UB}	819.26	$I + \Delta I_{UB}$

Table 1: Data for the ring-billed gull used in modelling

5. POWER EQUATIONS FOR INERTIAL DRAG

Assuming simple harmonic motion for the wing flapping, the power required for the downward acceleration phase is given by (Berg and Rayner 1995):

$$P_{iner-d-a} = 16 I \pi^2 f^3 \gamma^2 \tag{3}$$

The power in the downward deceleration phase is affected by aerodynamic braking. Some authors assume complete aerodynamic braking (Norberg 1990) whilst some assume zero aerodynamic braking (Berg and Rayner 1995). Studies by Burgess (Burgess 2014) showed that estimated that 50% aerodynamic braking occurs in the ring-billed gull at minimum power speed. Based on this assumption of 50% braking the inertial power for downward deceleration is given by:

$$P_{iner-d-d} = 8 I \pi^2 f^3 \gamma^2 \tag{4}$$

5.1 Upwards acceleration phase (u-a)

Taking into account 50% reduced inertia due to wing retraction in the upstroke gives the following:

$$P_{iner-u-a} = 8I\pi^2 f^3 \gamma^2 \tag{5}$$

5.2 Upwards deceleration phase (u-d)

Assuming a 50% reduction in planform area in the upstroke and assuming 50% aerodynamic braking during wing deceleration gives the following:

$$P_{iner-u-d} = 4I\pi^2 f^3 \gamma^2 \tag{6}$$

5.3 Average inertial power

The average inertial power during the whole flapping cycle is given by:

$$P_{iner-av} = 9I\pi^2 f^3 \gamma^2 \tag{7}$$

5.4 Minimum total power

The minimum total power is given by the empirical equation (Norberg 1990):

$$P_{min-power} = 50.2 m_b{}^{0.73} + \Delta P_{iner-av} \tag{8}$$

where m_b is the total mass of the bird and $\Delta P_{iner-av}$ is the increase in power due to the increase in wing inertia when the 4-bar mechanism is not present.

6.   RESULTS
6.1 Lower bound estimate of inertial power with no pantograph mechanism

Table 2 shows the lower bound power predictions for the gull flying at minimum power speed. The 4-bar mechanism has the effect of reducing the inertial power by 6.1% and reducing the total power needed by 0.6%. The power reduction from the 4-bar mechanism is small. However, when account is taken of the tight margins involved in the design of a flying vehicle, these figures show that the 4-bar mechanism gives a significant benefit.

Quantity	Phase	With 4-bar mechanism	Without 4-bar mechanism	Difference in power
$P_{iner-d-a}$ (W)	Down acceleration	3.54	3.74	
$P_{iner-d-d}$ (W)	Down deceleration	1.77	1.94	
$P_{iner-u-a}$ (W)	Up acceleration	1.77	1.85	
$P_{iner-u-d}$ (W)	Up deceleration	0.88	0.97	
$P_{iner-av}$ (W)	Av. inertial power	1.99	2.12	6.1%
$P_{min-total}$ (W)	Total power	23.40	23.53	0.6%
% inertia power of total power		8.5%	9.0%	

Table 2: Lower bound inertial power requirement with and without pantograph mechanism

6.2 Upper bound estimate of inertial power with no pantograph mechanism

Table 3 shows the upper bound power predictions for the gull flying at minimum power speed. The 4-bar mechanism has the effect of reducing the inertial power by 12.3% and the total power needed by 1.2%. Both these figures represent a significant reduction in power consumption.

Quantity	Phase	With 4-bar mechanism	Without 4-bar mechanism	Difference in power
$P_{iner-d-a}$ (W)	Down acceleration	3.54	3.91	
$P_{iner-d-d}$ (W)	Down deceleration	1.77	2.14	
$P_{iner-u-a}$ (W)	Up acceleration	1.77	1.96	
$P_{iner-u-d}$ (W)	Up deceleration	0.88	1.07	
$P_{iner-av}$ (W)	Av. inertial power	1.99	2.27	12.3%
$P_{min-total}$ (W)	Total power	23.40	23.68	1.2%
% inertia power of total power		8.5%	10.7%	

Table 3: Upper bound inertial power requirement with and without pantograph mechanism

7. DISCUSSION AND LESSONS FOR FLAPPING MICRO AIR VEHICLE (FMAV) DESIGN

7.1 Inertial power requirement

For the ring-billed gull the inertial power represented 8.5% of the total power for minimum power speed. The result shows that the inertial power requirement for flapping flight is significant for a medium-sized bird like a gull. This result is consistent with Berg and Rayner who studied a range of birds and estimated inertial power levels of between 6.4%-8.3% (when applying 50% conversion of kinetic energy to aerodynamic work). The reason for our slightly higher prediction is due to our analysis using a more recent equation for calculating flapping frequency (Pennycuick, 1996). This more recent equation gives a very slightly higher frequency for the gull and hence higher inertial energy requirement.

The significance of inertial drag means that it is important to reduce the wing inertia in FMAVs. Inertial power is proportional to wing inertia (from Equation **Error! Reference source not found.**) and so any reduction in the wing inertia will give a corresponding reduction in inertial power requirements.

7.2 Power savings produced by the 4-bar pantograph mechanism

At minimum power speed the model estimates that the 4-bar mechanism reduces the inertial power for the gull by 6.1% for the lower bound estimate and 12.3% for the upper bound estimate. This corresponds to a reduction in the total power of 0.6% for the lower bound estimate and 1.2% for the upper bound estimate. It should be noted that a 0.6% to 1.2% reduction in power corresponds to a 0.6% to 1.2% increase in range since range is inversely proportional to power. The overall power reduction (and increase in range) due to the presence of the 4-bar mechanism may appear small. However, when considering that every component of a flying machine must be highly optimised to reduce weight, the reductions are actually significant.

What is of importance is the 6.1%-12.3% reduction in the inertial power requirement. If every contribution to the power requirement in a bird is reduced by an average of 9% then the total power requirement is reduced by 9% (and range increased by 9%). In bird anatomy it is the case that virtually every component is specialised to reduce the power requirement. For example, birds

have special features to reduce weight such as thin-walled bones and high efficiency lungs (King, 1984) and recent work has shown how aerodynamic braking can actual help reduce inertial requirements (Burgess 2014). In aircraft design every component is specialised to reduce weight (Leland N.M. and Grant C.E. 2010). Therefore it is not surprising that there is a pantograph mechanism in the wings of birds that reduces the wing inertia.

8.   CONCLUSION
To conclude, this paper has shown that the energy-saving advantages of the 4-bar pantograph mechanism are desirable to replicate in a human-design FMAV. Not only does energy-saving result in a better power-to-weight ratio but it also increases the range of the vehicle. An additional advantage of the pantograph mechanism is that the wing is more compact and this allows the wings to be more slender and aerodynamically efficient. Some researchers have produced a bird-inspired pantograph mechanism for micro air vehicle design (Hara and Tanaka, 2007). Other researchers have produced a pantograph-type mechanism for hand rehabilitation robotics (Burton et al. 2011).

Our study shows that the pantograph mechanism has a significant effect in reducing the inertial power requirements of flapping flight. Our analysis confirms Norberg's assumption that the pantograph mechanism has a main function of reducing inertial power (Norberg 1990). However, there may be additional stability advantages with the 4-bar mechanism because it constrains the wrist and elbow joint to move together resulting in a more co-ordinated deployment and retraction of wings. These additional functionalities are yet to be fully investigated.

ACKNOWLEDGMENTS

NOMENCLATURE

b	Wing span (m)
C_L	Lift coefficient
C_w	Wing width (m)
I	Wing inertia $\times 10^{-6}$ (kgm^2) (with 4-bar mechanism)
I'_{LB}	Wing inertia $\times 10^{-6}$ (kgm^2) (without 4-bar mechanism) LB
I'_{UB}	Wing inertia $\times 10^{-6}$ (kgm^2) (without 4-bar mechanism) UB
f	Flapping frequency (Hz)
L_w	Length wing (m)
m_{b-t}	mass of biceps-triceps (kg)
m_w	Wing mass $\times 10^{-3}$ (kg)
m_{w-m}	mass of wrist muscles (kg)
r_{b-t}	radius of biceps-triceps (m)
r_{w-m}	radius of wrist muscle
S	Single wing area $\times 10^{-4}$ (m^2)
ω_{max}	Maximum angular velocity (rad/s)
ρ	Air density (kg/m^3)

REFERENCES

Berg, C. & Rayner, J., 1995. The moment of inertia of bird wings and the inertial power requirement for flapping flight. *J. Exp. Biol.*, 198(Pt 8), pp.1655–64.

Burgess, S.. et al., 2014. The effect of aerodynamic braking on the inertial power requirement of flapping flight: case study of a gull. *International Journal of Micro Air Vehicles*, 6(2).

Burgess, S.C. et al., 2011. A functional analysis of the jaw mechanism in the sling-jaw wrasse. *International Journal of Design & Nature and Ecodynamics*, 6(4), pp.258–271.

Burgess, S.C., 2007. Multi-functioning and multi-optimisation in feathers. *International Journal of Design & Nature*, 1(1), pp.1–10.

Burgess, S.C., King, A. & Hyde, R., 2006. An analysis of optimal structural features in the peacock tail feather. *Optics & Laser Technology*, 38(4-6), pp.329–334.

Burton, T.M.W. et al., 2011. Development of a parametric kinematic model of the human hand and a novel robotic exoskeleton. *IEEE ... International Conference on Rehabilitation Robotics : [proceedings]*, 2011, p.5975344.

Dumont, E.R., 2010. Bone density and the lightweight skeletons of birds. *Proceedings. Biological sciences / The Royal Society*, 277(1691), pp.2193–8.

Etoundi, A.C., Vaidyanathan, R. & Burgess, S.C., 2011. A bio-inspired condylar hinge joint for mobile robots. *2011 IEEE/RSJ International Conference on Intelligent Robots and Systems*, pp.4042–4047.

Hara, N. & Tanaka, K., 2007. Development of a flying robot with a pantograph-based variable wing mechanism. In *IEEE International Conference on Robotics and Automation*. pp. 349–354.

Meyers, R. a & Mathias, E., 1997. Anatomy and histochemistry of spread-wing posture in birds. 2. Gliding flight in the California gull, Larus californicus: a paradox of fast fibers and posture. *Journal of morphology*, 233(3), pp.237–47.

Norberg, U.M.L., 1990. *Vertebrate Flight: Mechanics, Physiology, Morphology, Ecology and Evolution* Zoophysiol., Springer-Verlag, Berlin, Germany.

Nudds, R.L., Dyke, G.J. & Rayner, J.M. V., 2007. Avian brachial index and wing kinematics: putting movement back into bones. *Journal of Zoology*, 272(2), pp.218–226.

Pennycuick, C., 1996. Wingbeat frequency of birds in steady cruising flight: new data and improved predictions. *J. Exp. Biol.*, 199(Pt 7), pp.1613–8.

Tobalske, B. & Dial, K., 1996. Flight kinematics of black-billed magpies and pigeons over a wide range of speeds. *Journal of Experimental Biology*, 280, pp.263–280.

Videler, J.J., 2005. *Avian Flight*, Oxford Ornithology Series. Oxford University Press.